

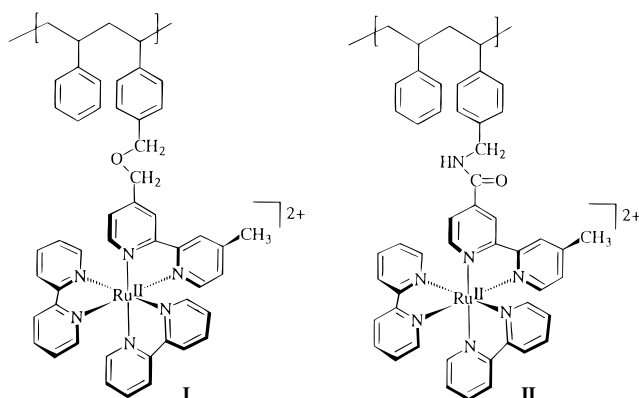
An Antenna Polymer for Visible Energy Transfer

Laurence M. Dupray, Martin Devenney,
Durwin R. Striplin, and Thomas J. Meyer*

Department of Chemistry, University of North Carolina
Chapel Hill, North Carolina 27590-3290

Received March 3, 1997

Derivatized polymers provide a versatile platform for creating multifunctional assemblies.¹ This includes polypyridyl complexes of Ru^{II} and Os^{II} which have high absorptivities in the visible based on metal-to-ligand charge transfer (MLCT) transitions.^{2,3} An early synthetic strategy for these involved attachment to polystyrene by an ether linkage (I). We have developed a new strategy based on amide linkage (II)³ and find that there is a dramatic difference between the two in their ability to promote intrastrand energy transfer.



The amide polymer was prepared from a 1:1 styrene-*p*-aminomethylstyrene copolymer of polydispersity 1.5 and an average of 16 repeat units.³ The amide link was formed by reaction with the acid-derivatized complexes, [M^{II}b₂b-COOH](PF₆)₂ (M = Ru, Os; b = 2,2'-bipyridine (bpy), b-COOH = 4'-methyl-2,2'-bipyridine-4-carboxylic acid) by using standard amide coupling conditions (see the Supporting Information).³ The resulting homopolymer samples are distributions, on the average, containing 16 complexes and abbreviated as [co-PS-CH₂NHCO-(M^{II}₁₆)](PF₆)₃₂ (M = Ru, Os). A mixed polymer was prepared by sequential coupling, first to the Os^{II} complex in limited amount (in a ratio of 3:16 relative to available amine sites on the polymer) with isolation and purification and then with the Ru^{II} complex in excess. This gave a polymer of average composition [co-PS-CH₂NHCO-(Ru^{II}₁₃Os^{II}₃)](PF₆)₃₂ (1). The derivatized polymers were purified and characterized by ¹H NMR, IR, UV-vis, and electrochemical measurements, as described previously.^{3,4} For example, for mixed polymer 1, waves for the Ru^{III/II} and Os^{III/II} couples appear at 1.30 and 0.87 V vs SCE in CH₃CN 0.1 M in [N(n-C₄H₉)₄](PF₆) having the expected relative peak currents of 13:3.

Transient resonance Raman measurements on an ether-linked model complex, [Ru^{II}b₂b-CH₂OBz](PF₆)₂ (b-CH₂OBz is 4-CH₂-

OBz-4'-CH₃bpy, Bz is benzyl) in acetonitrile, show that bpy is the acceptor ligand in the lowest MLCT excited state.⁵ Transient resonance Raman measurements (Supporting Information) on model complexes for the amide, [Ru^{II}b₂b-CONHBz](PF₆)₂ (b-CONHBz is 4-CONHBz-4'-CH₃bpy), [Ru^{II}(b-CONHBz)₃](PF₆)₂, [Ru^{II}b₃](PF₆)₂, and the polymer [co-PS-CH₂NHCO-(Ru^{II}₁₆)](PF₆)₃₂ in acetonitrile reveal that the acceptor ligand is the bpy-amide. This is shown by the appearance of resonantly enhanced bands for b-CONH- radical anion in the region 1000–1700 cm⁻¹ at 1594, 1550^a, 1492^a, 1442, 1428, 1332^a, 1286, 1208, 1195, 1127, and 1040 cm⁻¹ with 368.9 nm excitation and scattering (the superscript “a” denotes bands which overlap with neutral ligand bands). On the basis of structure II and the results of molecular modeling,⁴ this means that the excited-state dipole is aligned along the amide ligand oriented toward the polymer backbone and nearest neighbor complexes.

In the ether-linked polymer, [co-PS-CH₂OCH₂-(Ru^{II}₂₂Os^{II}₅)](PF₆)₅₄ (2), energy transfer from Ru^{II}* to Os^{II} is favored by 0.36 eV and occurs rapidly with $k > 2 \times 10^8 \text{ s}^{-1}$ ($\tau < 5 \text{ ns}$) in acetonitrile solution at room temperature. However, energy migration by Ru^{II}* to Ru^{II} self-exchange is slow ($\tau > 1 \mu\text{s}$, $k < 1 \times 10^6 \text{ s}^{-1}$).⁴

In mixed polymer 1, there is evidence for both facile energy transfer and migration in deaerated acetonitrile at room temperature. This is shown in the emission spectra in Figure 1. These spectra demonstrate that excitation at 460 nm, where Ru^{II} is the dominant light absorber (Figure 2), results in nearly complete Ru^{II}* quenching compared to [co-PS-CH₂NHCO-(Ru^{II}₁₆)](PF₆)₃₂ (3). There is clear evidence for emission from Os^{II}* as shown by comparison with [co-PS-CH₂NHCO-(Os^{II}₁₆)](PF₆)₃₂ (4). Emission quantum yields for 3 and 4 are $\phi_{\text{Ru}^{II*}} = 5.0 \times 10^{-2}$ and $\phi_{\text{Os}^{II*}} = 4.6 \times 10^{-3}$.³ The efficiency of Ru^{II}* to Os^{II} energy transfer is $\eta_{\text{en}} = 0.94 \pm 0.08$ in acetonitrile solution at room temperature with 420 nm excitation, 0.98 with 460 nm excitation, and 0.92 with 500 nm excitation. These values were calculated by using eq 1. A_{Os} and A_{Ru} are the absorbances of Os^{II} and Ru^{II} at the excitation wavelength and I_{RuOs} and I_{Ru} are the integrated emission intensities for 1 and 3.^{6,7} In solutions containing comparable concentrations of homopolymers 3 and 4, there is no evidence for Ru^{II}* quenching.

$$\eta_{\text{en}} = \frac{A_{\text{Os}}}{A_{\text{Ru}}} \left[1 - \frac{I_{\text{RuOs}}}{I_{\text{Ru}}} \right] \quad (1)$$

Time-dependent emission and absorption measurements reveal that net energy transfer is rapid with Os^{II}* completely formed during the laser pulse of the apparatus used (5 ns). Emission decay at 800 nm, where Os^{II}* is the sole emitter, occurs with $\tau = 65 \text{ ns}$ ($k = 1.54 \times 10^7 \text{ s}^{-1}$), the lifetime obtained for Os^{II}* in homopolymer 4.³ The decay of the small amount of residual Ru^{II}* emission (<2%), monitored at 600 nm where only Ru^{II}* emits, is nonexponential.⁹

On the basis of the results of molecular modeling calculations, these polymers have extended spatial structures dominated by the large (~14 Å diameter) metal complex dications.⁴ For the ether-linked polymers, the average spacing between the peripheries of nearest neighbor complexes is ~7 Å and that between

(1) (a) Guillet, J. *Polymer Photophysics and Photochemistry*; Cambridge University Press: Cambridge, U.K., 1985. (b) Stoessel, S. J.; Stille, J. K. *Macromolecules* **1992**, *25*, 1832. (c) Webber, S. E. *Chem. Rev.* **1990**, *90*, 1469. (d) Baxter, S. M.; Jones, W. E.; Danielson, E.; Worl, L. A.; Younathan, J.; Strouse, G. F.; Meyer, T. J. *Coord. Chem. Rev.* **1991**, *111*, 47. (e) Jones, W. E.; Watkins, D. M.; Fox, M. A. *Chem. Eng. News* **1993**, *71* (11), 38.

(2) (a) Younathan, J. N.; McClanahan, S. F.; Meyer, T. J. *Macromolecules* **1989**, *22*, 1048. (b) Margerum, L. D.; Meyer, T. J.; Murray, R. W. *J. Phys. Chem.* **1986**, *90* (12), 2696.

(3) Dupray, L. M.; Meyer, T. J. *Inorg. Chem.* **1996**, *35* (21), 6299.

(4) Jones, W. E.; Baxter, S. M.; Strouse, G. F.; Meyer, T. J. *J. Am. Chem. Soc.* **1993**, *115*, 7573.

(5) The excited-state resonance Raman spectrum in CH₃CN with 368.9 nm excitation and scattering is essentially identical with [Ru(bpy)₃]²⁺.*

(6) (a) Holden, D. A.; Guillet, J. *Macromolecules* **1980**, *13*, 289. (b) Schiller, P. W. In *Biochemical Fluorescence*, Chen, R. F., Edelhoch, H., Eds.; Marcel Dekker: New York, 1975; Vol. 1, pp 285–303.

(7) The separate Ru^{II}* and Os^{II}* emissions in [co-PS-CH₂NHCO-(Ru^{II}₁₃-Os^{II}₃)](PF₆)₃₂ were deconvoluted by application of a Frank-Condon-based spectral fitting procedure to each component⁸ and constructing the combined emission profile from 500 to 1200 nm.

(8) Claude, J. P. Ph.D. Dissertation, University of North Carolina, Chapel Hill, NC, 1995.

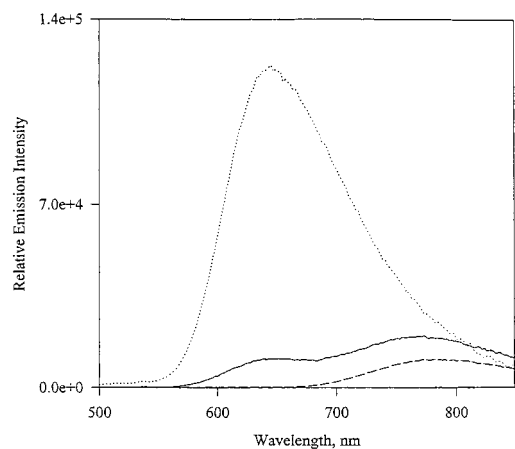


Figure 1. Emission spectra of $[co\text{-PS-CH}_2\text{NHCO-(Ru}^{\text{II}}_{13}\text{Os}^{\text{II}}_3)](\text{PF}_6)_{32}$ (—), $[co\text{-PS-CH}_2\text{NHCO-(Ru}^{\text{II}}_{16})](\text{PF}_6)_{32}$ (⋯), and $[co\text{-PS-CH}_2\text{NHCO-(Os}^{\text{II}}_{16})](\text{PF}_6)_{32}$ (- - -) (460 nm excitation) in deaerated acetonitrile at room temperature. Emission profiles for the Ru^{II} and Os^{II} homopolymers have been scaled to their relative emission quantum yields.

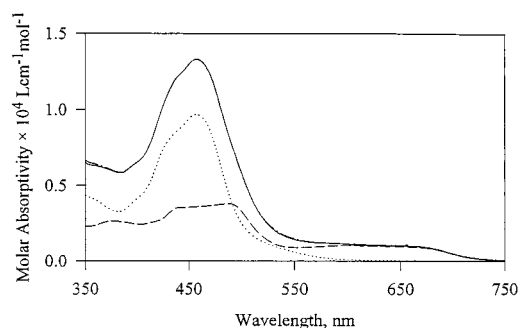
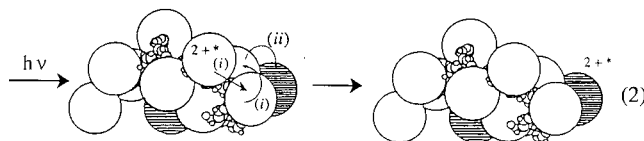


Figure 2. Absorption spectra of $[co\text{-PS-CH}_2\text{NHCO-(Ru}^{\text{II}}_{13}\text{Os}^{\text{II}}_3)](\text{PF}_6)_{32}$ (—), and a mixture of $[co\text{-PS-CH}_2\text{NHCO-(Ru}^{\text{II}}_{16})](\text{PF}_6)_{32}$ and $[co\text{-PS-CH}_2\text{NHCO-(Os}^{\text{II}}_{16})](\text{PF}_6)_{32}$ in molar ratio 13:3 (- - -), in CH_3CN at room temperature. The two spectra are nearly completely overlapped. The spectra of the separate Ru^{II} (⋯) and Os^{II} (- - -) homopolymers at a 13:3 ratio are also shown.

non-nearest neighbors is $\sim 21 \text{ \AA}$. On the basis of the loading statistics, $\sim 1/2$ of the Ru^{II} sites on the backbone are not adjacent to Os^{II} . As illustrated in eq 2, with the open spheres representing Ru^{II} and the cross-hatched spheres representing Os^{II} , net energy transfer from $\text{Ru}^{\text{II}*}$ to Os^{II} requires two processes: $\text{Ru}^{\text{II}*}$ to Ru^{II} energy migration (k_i in eq 2), for which $\Delta G^\circ = eV$, and the

actual energy transfer step (k_{ii} in eq 2) for which $\Delta G^\circ = -0.36 \text{ eV}$. On the basis of our results, $k > 2 \times 10^8 \text{ s}^{-1}$ for both migration and transfer.



For ether-linked polymer **2**, $k_{ii} > 2 \times 10^8 \text{ s}^{-1}$ but energy migration is slow with $k_i < 1 \times 10^6 \text{ s}^{-1}$.⁴ This is a dramatic difference apparently caused by the difference in orientation of the excited-state dipole. The excited-state resonance Raman results show that the dipole is oriented away from the backbone in **2** and toward the backbone in amide-linked polymer **1**. The mechanism of energy transfer may be through space (Förster) or through bond (Dexter), or a combination of the two. In either case, orientation toward the backbone decreases the distance to adjacent chromophores enhancing the rate of energy transfer. The resulting enhancement in k_i of >200 provides a dramatic example of the use of substituent effects to control supramolecular dynamics.

The amide-linked polymers are polychromophoric arrays and intense visible light absorbers with $\epsilon = 214\,000 \text{ L cm}^{-1} \text{ mol}^{-1}$ per average strand at the absorption maximum of 458 nm for **1**. Intrastrand energy transfer is highly efficient with energy migration ($\tau < 5 \text{ ns}$) occurring >200 times faster than excited-state decay ($\tau_M = 910 \text{ ns}$).³ This opens the possibility of using suitably derivatized polymers as visible light collectors and antenna for sensitizing photoinduced electron transfer, as occurs in the photosynthetic apparatus of green plants.¹⁰

Acknowledgment. We thank the Department of Energy under Grant DE-FG05-86ER13633 for support of this research.

Supporting Information Available: Descriptions of the syntheses of the mixed metallopolymer and transient resonance Raman measurements (2 pages). See any current masthead page for ordering and Internet access instructions.

JA970660C

(9) These emission decays could be fit to the biexponential decay function, $I(t) = a \exp(-k_1 t) + (1 - a) \exp(-k_2 t)$, with $I(t)$ the emission intensity at time t , $k_1 = 4.4 \times 10^7 \text{ s}^{-1}$ ($a = 0.78$), and $k_2 = 6.9 \times 10^6 \text{ s}^{-1}$ in CH_3CN at room temperature. We assume that this emission is from a small fraction of partially quenched $\text{Ru}^{\text{II}*}$ sites. The average lifetime, τ_M , calculated from, $\tau_M = a k_1 + (1 - a) k_2$ was 50 ns compared to $\tau_M = 910 \text{ ns}$ for pure homopolymer **3** under the same conditions.³

(10) (a) Tomita, G.; Rabinovitch, E. *Biophys. J.* **1962**, *2*, 483. (b) Porter, G.; Treadwell, C. J.; Searle, G. F.; Barber, J. *Biophys. Acta* **1978**, *501*, 232.